Composites Science and Technology 210 (2021) 108839

Contents lists available at ScienceDirect

Composites Science and Technology

journal homepage: www.elsevier.com/locate/compscitech

Damage detection of CFRP composites by electromagnetic wave nondestructive testing (EMW-NDT)

Qing-Qing Ni [a,b,1,*], Jun Hong [c,d,1], Ping Xu [c], Zhenzhen Xu [d,**], Kirill Khvostunkov [e], Hong Xia [b]

[a] Key Laboratory of Advanced Textile Materials and Manufacturing Technology Ministry of Education, Zhejiang Sci-Tech University, Hangzhou, 310018, Zhejiang, China
[b] Department of Mechanical Engineering & Robotics, Shinshu University, Ueda, 386-8567, Japan
[c] Interdisciplinary Graduate School of Science and Technology, Shinshu University, Ueda, 386-8567, Japan
[d] College of Textile and Garments, Anhui Polytechnic University, Wuhu, Anhui, 241000, China
[e] Faculty of Mechanics and Mathematics, Lomonosov Moscow State University, Moscow, Russia

ARTICLE INFO

Keywords:
Carbon fibers
Defects
Non-destructive testing
Delamination
Crack

ABSTRACT

Damages such as fiber breakage and delamination are likely to occur inside CFRP composites when subjected to external forces, such as impact and fatigue load. These damages are mostly invisible and cause safety hazards during the service of the products. This study proposes a new type of nondestructive testing (NDT) method using electromagnetic wave (EMW) technique, EMW-NDT. It was proven that the proposed EMW-NDT method is effective in detecting damages such as delamination, crack or other defects in CFRP composites. The EMW-NDT method's detection capacity to the delamination size, delamination thickness, and slits in CFRP composites was investigated. A reasonable sensitivity to the damage volume change in delamination was confirmed with a damage area ratio of 12.6%/dB and a thickness change of 5.5 dB/mm. It was found that the incident angle of the EM wave plays a vital role in detecting sensitivity because of the skin effect in CFRP composites. The results confirmed that the proposed method demonstrates good detection sensitivity to delamination size and thickness. In terms of crack damage, the slit and its length were detected and the slit direction was successfully identified in this study based on the characteristics of the electromagnetic interference (EMI) shielding anisotropy in CFRPs. Moreover, the proposed EMW-NDT method with specified designed free-space measurement system is contactless, and no coupling medium is required; thus, it exhibits huge potential to be widely used as a new damage detection technique for CFRP composites.

1. Introduction

Carbon-based composites have been widely used in various industries [1–3] due to their high mechanical and electrical performances [4,5]. Specifically, carbon fiber reinforced polymer (CFRP) composites have been widely used to replace high-density metal materials [6,7], due to their high elastic modulus and strength to weight ratio as well as their excellent corrosion resistance. The application of CFRP include aircraft, wind turbines, automobiles, and sports items such as bicycles, skis, and rowing boats [8]. With the diversification of CFRP applications, its production process has become fairly complicated. Many defects and damages will appear in the production and application processes. For example, unevenness of resins and appearance of voids will occur during the production process, and the material will crack and delaminate after being impacted in the application process [9,10]. The presence of these defects will significantly affect the performance and application of the CFRP materials, with the delamination and crack damage in the composite materials particularly difficult to detect, leading to hidden safety hazards during use. Therefore, carrying out nondestructive testing (NDT) is essential to evaluate the various damage to CFRPs during their production and service.

A number of NDT methods currently exist for detecting the defects and damage within composite materials. Among them, the eddy current testing method has been extensively studied. This is a noncontact method mainly used to detect cracks and corrosion in high conductivity materials [11,12]. To improve the damage detection in CFRPs, Wu et al.

* Corresponding author. Key Laboratory of Advanced Textile Materials and Manufacturing Technology Ministry of Education, Zhejiang Sci-Tech University, Hangzhou, 310018, Zhejiang, China.
** Corresponding author. College of Textile and Garments, Anhui Polytechnic University, Wuhu, Anhui, 241000, China.
E-mail addresses: niqq@shinshu-u.ac.jp (Q.-Q. Ni), xuzhenzhen@ahpu.edu.cn (Z. Xu).
[1] co-first author, these authors contributed to this work equally.

https://doi.org/10.1016/j.compscitech.2021.108839
Received 13 December 2020; Received in revised form 8 March 2021; Accepted 27 April 2021
Available online 1 May 2021

developed a T-R probe with a special structure, to overcome the impact of lift-off variation and detected the defects within CFRPs [13]. A novel wireless power transfer-based eddy current NDT using a flexible printed coil array has been proposed by L. U. Daura et al. [14], which can be used for the eddy current testing (ECT) of pipeline sample. Elsewhere, Mizukami et al. designed and changed the probe geometry of the eddy current testing setup to improve the sensitivity to delamination in CFRPs, with a delamination with a length and width of 10 mm consequently observable [15]. Meanwhile, He et al. found that the defects induced by a low-energy impact can be effectively detected via scanning pulsed eddy current testing [16]. Many researchers also studied the application of eddy current testing in CFRP examination through modeling [17,18]. Due to the electrical performance requirements in the eddy current testing method, the method is not mature in the terms of CFRP testing. At the same time, the method also exhibits certain other disadvantages, such as the limitation of the penetration depth and the unsuitability for the detection of complex geometries and large area products.

Another prevalent and widely used NDT method is the ultrasonic testing method, which has mainly been used to detect material delamination. The ultrasonic C-scan technique can identify the location, orientation, and size of defects. Many research reports demonstrated the use of ultrasonic NDT for the detection of impact damage in CFRPs [19–21]. However, a number of disadvantages remain in using the ultrasonic NDT method. For example, a medium is required to transmit ultrasonic energy from the probe to the material, such as water and gel, and detecting the delamination that exists near the surface of the material is not easy [15,22]. While a relatively new ultrasonic NDT has been developed which involves noncontact without the requirement of a coupling medium, the method exhibits many limitations and must be performed under specific conditions [23,24].

Meanwhile, in terms of other methods, while shearography [25,26] and radiographic testing [27,28] methods have been applied to the examination of CFRP materials, these also involve certain limitations, such as being only applicable to the detection of particular specimens and being limited to certain types of damage [29]. The infrared thermography method can be used to detect defects through monitoring the temperature variations caused by the discontinues in the material [30]. R. Sutthaweekul et al. [31] proposed a novel application of microwave NDT to detect and characterize the flat-bottom hole (FBH) defect in coated glass fiber reinforced plastics (GFRP) pipes. Numerous works [32–34] focused on the application of thermal imaging technology in relation to composites, with the cost of the machine and the hot spots where reflective surfaces are prone to error found to limit its full application.

Free-space measurement is generally used to determine the magnetic permeability and electric permittivity of materials and can be conducted under different temperature conditions [35,36]. A number of research works demonstrated the possibility of applying a free-space method, to detect hardened cement specimens [37] and to determine the dispersion and orientation of the fiber that exists in concrete [38]. However, few reports focused on the application of the EM wave technique as a nondestructive testing of CFRP for evaluate CFRP damage.

Due to the high electrical conductivity of carbon fiber, CFRPs always achieve an excellent electromagnetic interference (EMI) shielding performance. When a damage occurs inside CFRP composites, the single-layer composite material will become a regional “double-layer” or “multi-layer” material, where the air layer is formed. Multiple reflections will occur when the EM wave passes through these regions, resulting in changes to the transmission coefficient. The damage inside the CFRP could be detected through analyzing and comparing the difference in transmission coefficient. In the present paper, a new type of NDT method using electromagnetic wave (EMW-NDT) is proposed to detect the damage in CFRP composites. The inspection ability of this method in relation to the different types of damages inside CFRP composites is investigated. The EMW-NDT present a noncontact and nondestructive measurement method, wherein a coupling medium is not required. This method allows for testing samples of large sizes with various shapes, and the test process is quick where the testing results could be obtained in few seconds. As the electrical conductivity of CFRP was affected by the carbon fiber direction [39,40], the detection performance of the EM wave technique at the different angles of incident EM wave between the electric field of the EM waves and carbon fiber direction was analyzed. The experimental results indicated that the proposed EMW-NDT method is effective in detecting damage such as delamination, crack or other defects in CFRP composites.

2. Experimental

2.1. Sample preparation

The CFRP samples were fabricated from unidirectional prepreg sheets. The delamination damage was reproduced by inserting Teflon film between the CFRP layers. The main reason for choosing Teflon film is its high electrical resistance (almost insulation) and dielectric constant value (≈2.1), which is close to that of air (≈1). Slits in the CFRPs were prepared using a knife. The sample dimension was 250 mm in length and 250 mm in width. All the CFRP composites were cured using a hot press machine at 135 °C, 2 MPa for 1.5 h, as shown in Fig. 1.

Carbon prepregs sheets (NT81250-525S) with an areal density of 125 g/m^2 were supplied by Nippon Graphite Fiber Corporation, while the Teflon film was purchased from Nitto Denko Corporation, with the intrinsic properties listed in Table 1.

2.2. EMW-NDT measurement

To measure the changes in electromagnetic performance for detecting damages inside the CFRP, the electric field of the incident EM waves was linearly polarized. As shown in Fig. 2(a), the free-space setup consisted of transmitting and receiving horn antennas connected to a vector network analyzer by two coaxial cables. A pair of dielectric lenses was mounted between the transmitting and receiving antennas. The upper lenses demonstrated the capacity to convert the spherical EM wave emitted by the transmitting antenna into a linearly polarized plane wave. After the sample shielded the EM wave, the remaining EM waves were converted and focused by the bottom lens, and the converging beam ultimately reached the receiving antenna. The presence of the lens reduced the multiple reflections between the transmitting antenna and the sample as well as the diffraction around the sample, which significantly improved the accuracy of the test results.

A sample stage between the two antennas was present, which was used for the placement of the sample during the test. Since the free-space setup was placed vertically, no fixture was required to secure it. An aperture was used in the middle of the sample stage, with the measured part of the sample placed within the aperture range. We prepared sample stage with aperture diameters of 16 cm. To avoid the impact of edge effects and multiple reflections, the device was required to be calibrated prior to the measurement. The maximum size of specimen that can be tested by this method depends on the sample stage size, the distance between antennas, and other related parameters. The device could be suitable for the detection of large-size composite structures through proper modification.

The transmission scatter parameters (S_{21}) (Fig. 2(b)) was recorded by the vector network analyzer at the frequency range of 5–15 GHz (Fig. 2

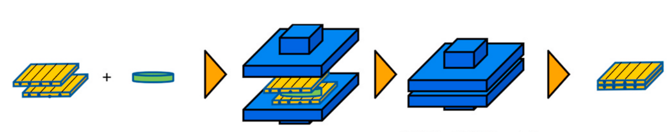

Fig. 1. Fabrication process of CFRP composites inserted with Teflon film.

Table 1
Properties of the Teflon film used in this study.

Profile	Value	Unit
Thickness	0.05	mm
Permittivity	2.1	–
Volume Resistivity	over 1×10^{17}	Ω•cm

(b)). The attenuation of the EM wave was defined as the shielding effectiveness (SE), which could be calculated using the following equations:

$$SE = S_{21}(dB) = -10\log\left(|S_{21}|^2\right) \tag{1}$$

while the detection sensitivity ΔS_{21}(dB) can be defined as follows:

$$\Delta S_{21}(dB) = \left|S'_{21}(dB) - S_{21}(dB)\right| \tag{2}$$

where S'_{21}(dB) and S_{21}(dB) are the transmission coefficient of CFRP with and without damage, respectively.

The electrical conductivity of CFRP is affected by the direction of the carbon fiber, i.e., the angle between the fiber direction and the electric field direction of the incident EM wave will affect the transmission coefficient. To ascertain the optimum incident angle of the EM wave for the best detection sensitivity of damage within CFRPs, the samples were evaluated using three typical incident angles of 0°, 45° and 90° as shown in Fig. 2(c).

3. Results and discussion

3.1. Electromagnetic interference shielding theory

According to the multimedia shielding theory [41], the transmission coefficient T of n-layer materials (Fig. 3(a)) for the H-field is:

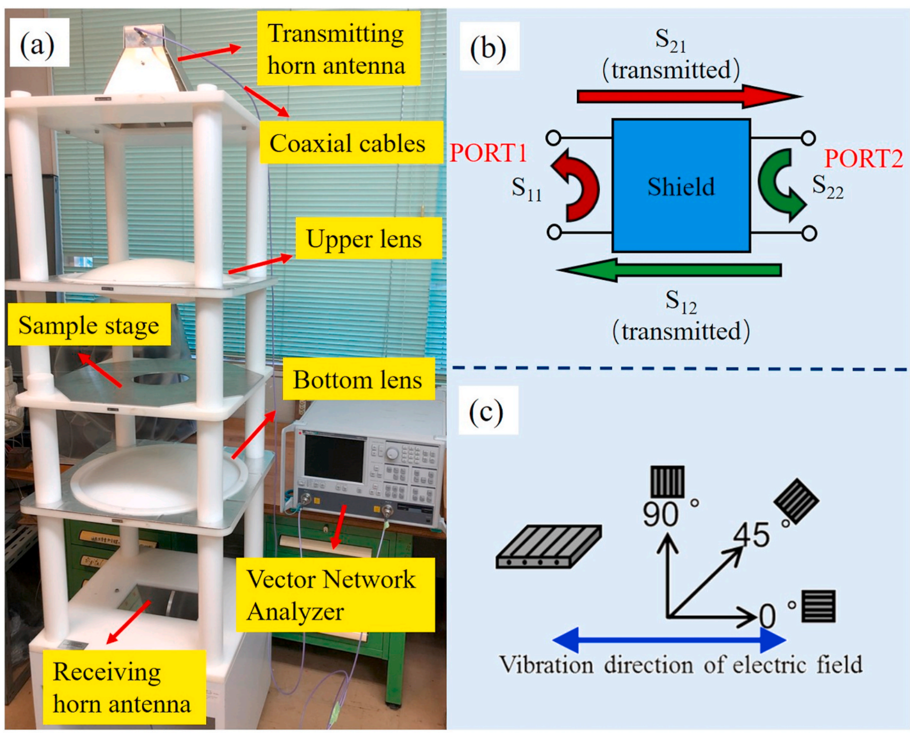

Fig. 2. (a) The specially designed free-space measurement system and its set-up, (b) illustration of the S-parameter obtained via measurement, (c) incident angle of the EM wave between fiber direction and electric field direction.

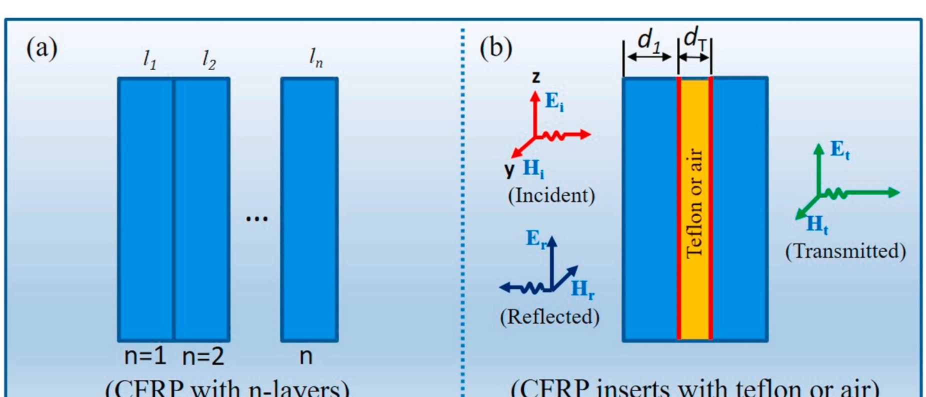

Fig. 3. CFRP with different structures: (a) n-layers CFRP; (b) CFRP separated by Teflon film or air.

$$T = p\left[\left(1-q_1e^{-2r_1l_1}\right)\left(1-q_2e^{-2r_2l_2}\right)\cdots\left(1-q_ne^{-2r_nl_n}\right)\right]^{-1}\times e^{-r_1l_1-r_2l_2-\cdots-r_nl_n} \tag{3}$$

Meanwhile, the total shielding SE_T, absorption SE_A, reflection SE_R, and the multiple reflection SE_M are expressed as follows:

$$SE_T = SE_A + SE_R + SE_M = 20log_{10}|T| \tag{4}$$

$$SE_A = 20log_{10}\left|e^{-r_1l_1-r_2l_2\cdots-r_nl_n}\right| \tag{5}$$

$$SE_R = 20log_{10}|P| = 20log\left|\frac{2\eta_0\cdot 2\eta_1\cdot\cdot 2\eta_n}{(Z_w+\eta_1)(\eta_1+\eta_2)\cdot\cdot(\eta_n+Z_w)}\right| \tag{6}$$

$$SE_M = 20log_{10}\left[\left(1-q_1e^{-2r_1l_1}\right)\left(1-q_2e^{-2r_2l_2}\right)\cdots\left(1-q_ne^{-2r_nl_n}\right)\right]^{-1} \tag{7}$$

where q is the reflection coefficient, p is the transmitted coefficient, l is the shield thickness, η is the intrinsic impedance of the shield, Z_W is the EM wave impedance, and r is the propagation constant.

$$r = \sqrt{\iota\omega\mu(\sigma+\iota\omega\iota)} \tag{8}$$

$$q_n = \frac{(\eta_n-\eta_{n-1})(\eta_n-Z_W)}{(\eta_n+\eta_{n-1})(\eta_n+Z_W)} \tag{9}$$

For a single layer CFRP with thickness d and intrinsic impedance Z_B, the shielding effectiveness (SE_S) can be expressed as follows:

$$\begin{aligned} SE_S &= 20log_{10}|T| \\ &= SE_A + SE_R + SE_M \\ &= 20\log_{10}\left(e^{-rd}\right) + 20\log\left|\frac{2Z_w\cdot 2Z_B}{(Z_w+Z_B)(Z_B+Z_w)}\right| + 20\log\left|1-qe^{-2rd}\right| \\ &= 8.68\frac{d}{\delta} + 20\log_{10}\frac{|K+1|^2}{4|K|} + 20\log_{10}\left|1-\frac{(K-1)^2}{(K+1)^2}e^{-2rd}\right| \end{aligned} \tag{10}$$

where k is the ratio between the EM wave impedance (Z_W) and intrinsic impedance (Z_B) of CFRP, while δ is the skin depth, as below:

$$\delta = 1\Big/\sqrt{\pi\mu f\sigma} \tag{11}$$

where μ is magnetic permeability, f is frequency, and σ is electrical conductivity.

For a CFRP with Teflon or air inserts (Fig. 3(b)), it will be imaged as a multi-layer structure with n = 3, with the thickness d_1, half that of single CFRP (d). The thickness of Teflon or air are d_T. According to Eq. (4), the SE value of CFRP with Teflon film or air (SE_d) can be rewritten follows:

$$\begin{aligned} SE_d &= 20log_{10}\left(e^{-rd_1-r_td_T-rd_1}\right) + 20log\left|\frac{2Z_w\cdot 2Z_B\cdot 2Z_T\cdot 2Z_B}{(Z_w+Z_B)(Z_B+Z_T)(Z_T+Z_B)(Z_B+Z_w)}\right| \\ &+20log\left|\left(1-q_1e^{-2r_1d_1}\right)\left(-q_2e^{-2r_2d_T}\right)\left(-q_3e^{-2r_1d_1}\right)\right| \\ &= 8.68\frac{d_1+d_2}{\delta} + 20\log_{10}\frac{|K+1|^2}{4|K|} + 20\log_{10}\frac{|K_1+1|^2}{4|K_1|} \\ &+20\log\left|\left(1-q_1e^{-2r_1d_1}\right)\left(-q_2e^{-2r_2d_T}\right)\left(-q_3e^{-2r_1d_1}\right)\right| \end{aligned} \tag{12}$$

To discuss the effect of Teflon/air on the EMI shielding performance of CFRP, we compared the SE value of CFRP with/without Teflon/air. Here, the detection sensitivity, $\Delta S_{21}(dB)$, could be expressed as follows:

$$\begin{aligned} \Delta S21(dB) &= SEd - SEs \\ &= 20\log_{10}\frac{|K_1+1|^2}{4|K_1|} + 20log\left|\left(1-q_2e^{-2r_2d_T}\right)\right| \end{aligned} \tag{13}$$

where Z_T is the impedance of Teflon or air.

In this study, $d = 0.55 \times 10^{-3}$ m, $d_1 = d_2 = d/2 = 0.275 \times 10^{-3}$ m, and the electrical conductivity σ of CFRP at the test degree 45° was 453 S/m. Then, the detection sensitivity ΔS_{21}(dB) for the CFRP with Teflon and air at 10 GHz were 4.6 and 5.7 dB. This indicated that the insertion of Teflon film in CFRP can improve the shielding performance of the material, which means that the delamination damage inside the CFRP could be detected by comparing the transmission coefficient value changes. Simultaneously, the theoretical analysis results also indicated that the EMI shielding effectiveness was similar to that of the CFRP inserted with air or Teflon film.

3.2. Detection sensitivity of delamination damage size by ΔS_{21} (dB)

To accurately predict the service life of CFRPs, the ability to quantitatively characterize any delamination defects via NDT technology is essential. The delamination size is a main factor affecting the CFRP's service life, meaning detecting the delamination area is critical in the NDT process. The CFRP with delamination areas of Φ 5 cm in diameter was reproduced by inserting Teflon film. The samples were square shaped with a side length of 25 cm, as shown in Fig. 4(a), with the measurement involving the sample stage of a Φ16 cm diameter aperture.

Fig. 4(b) shows the S_{21}(dB) values of CFRP at the incident angle of 0°. With the change in Teflon area inside the CFRP, the S_{21}(dB) value changed at specific frequencies; however, the differences in S_{21}(dB) were not large enough to distinguish the delamination area. Fig. 4(c) and (d) show the S_{21}(dB) values of the CFRP at the testing angle of 45° and 90°, respectively. A detectable difference in S_{21}(dB) values was obtained within the entire frequency range of 5–15 GHz. Here, it was clear that the existence of delamination led to an increase in the SE values of the CFRP. Then, with the delamination damage created inside the CFRP composites, the single-layer CFRP composite was split into a "double-layer" version, and the air zone was formed. Multiple reflections would occur when the EM wave passed through these regions, resulting in the improvement of the EMI shielding performance, which was consistent with the shielding theory analyzed in the previous section.

The variation in SE value is shown in Table 2. The lower detection sensitivity of delamination at the 0° incident angle was deemed to be due to the small skin depth for CFRP at the fiber direction. Eq. (11) indicates that the skin depth decreases with the increase in frequency and electrical conductivity. Due to the anisotropy of the electrical conductivity of unidirectional CFRP, this material exhibits the highest electrical conductivity at the fiber direction, resulting in the smallest skin depth. For example, the skin depth of CFRP at 10 GHz was around 0.0459 mm in the fiber direction (0°), as shown in Table 2. According to the definition of skin depth, at a 0° incident angle where the electric field is consistent with the fiber direction, the EM wave strength would be reduced to 1/e of its incident strength before the EM wave is transmitted out the CFRP composites. That is, most of the EM wave cannot reach the depth of the delamination area, resulting in a small detection sensitivity. At the 10 GHz frequency, the skin depth was calculated to be 0.742 mm at the 45° incident angle and 1.221 mm at the direction perpendicular to the carbon fiber (90°), which are far larger than its thickness (0.55 mm). Consequently, the penetration ability of the EM wave to the CFRP was improved as the incident angle testing angle to fiber orientation increased, and the delamination size was detected at the incident angles of 45° and 90°, which is shown in Fig. 4(c) and (d). Here, the delamination area ratio is about 9.8%, then the detection sensitivity of the damage area ratio was around 12.6%/dB at the 45° incident angle.

As Fig. 5(c) shows the detection sensitivity value increased with the increment of the delamination size. The detection ability at the 45° incident angle is better than that at the 90° angle, and they. The detection sensitivity of the delamination area at the 45° and 90° can be predicted approximately as follows:

$$\Delta S_{21}(dB) = 0.093\times d + 0.27 \text{for the } 45^\circ \text{ incident angle} \tag{14}$$

$$\Delta S_{21}(dB) = 0.082\times d + 0.26 \text{for the } 90^\circ \text{ incident angle} \tag{15}$$

The predicted results are in good consistent with the experimental, as

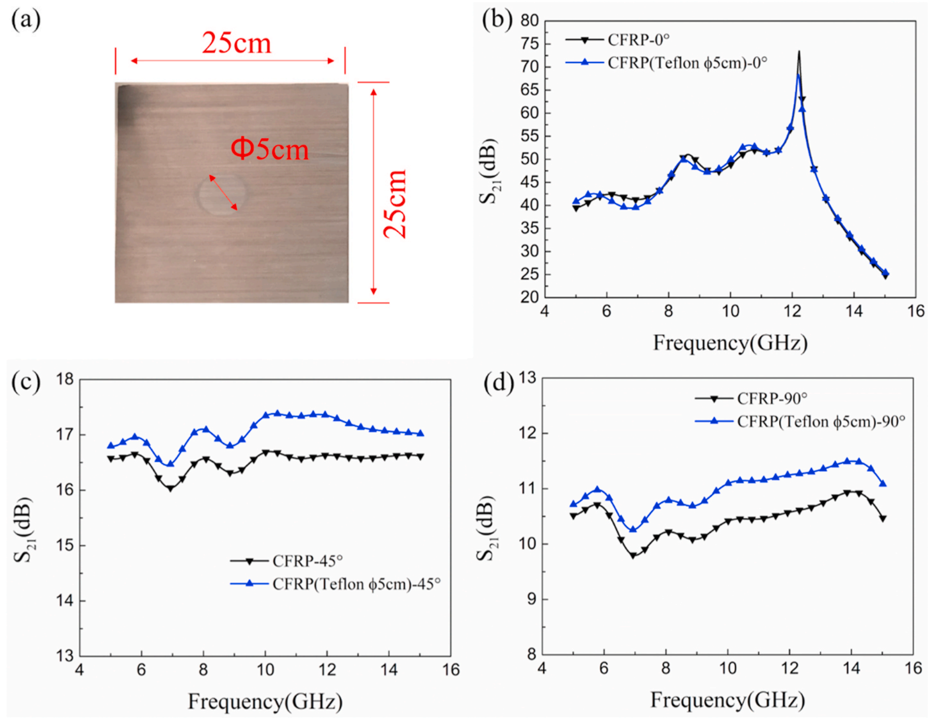

Fig. 4. (a) Images of CFRP inserts of Teflon with different diameters; S_{21}(dB) values of CFRPs inserted with 5 cm diameter Teflon film under three typical incident angles of (b) 0°, (c) 45° and (d) 90°.

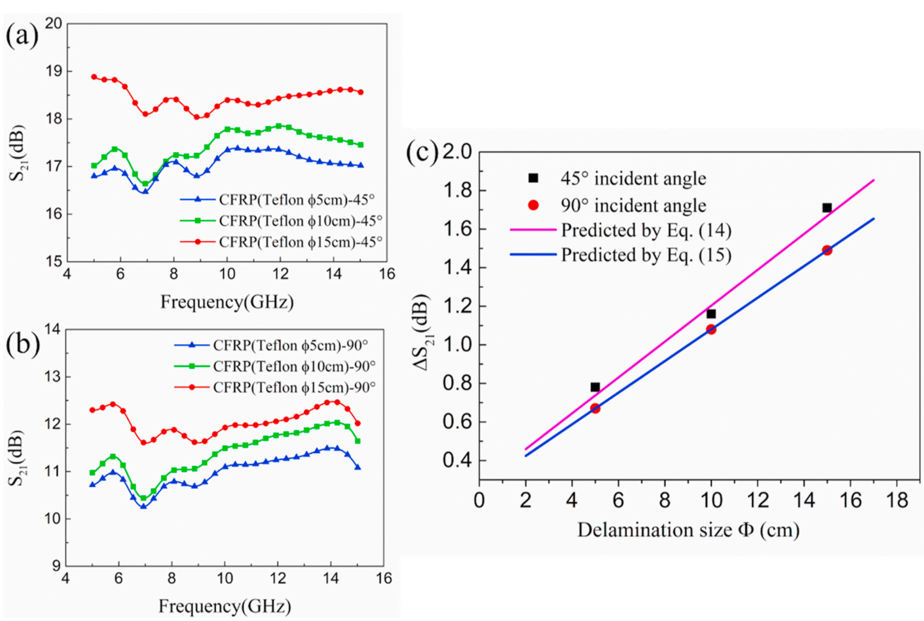

Fig. 5. (a) (b) S_{21}(dB) values of CFRPs inserted with various diameters of Teflon film under the testing angles of 45° and 90°; (c) detection sensitivity at 10 GHz; The influence of delamination size on the detection sensitivity was investigated by changing the delamination areas reproduced by inserting Teflon films with different diameters (Φ5, Φ10 and Φ15cm). These were remarked as CFRP (Teflon Φ5cm), CFRP (Teflon Φ10cm) and CFRP (Teflon Φ15cm), and they exhibited delamination areas of 9.8%, 39% and 87.9%, respectively. Fig. 5(a) and Fig. 5(b) show the relationship between the variation in SE value and the delamination area at the incident angles of 45° and 90°, respectively. The greater the delamination areas, the more EM waves were attenuated due to the delamination damage in the CFRP composites. This means that the delamination size could be detected using the proposed EMW-NDT method.

Table 2
Skin depth and detection sensitivity ΔS_{21}(dB) of CFRPs with different incident angles at 10 GHz.

Incident angle of EM wave	0°	45°	90°
Skin depth δ (mm)	0.0459	0.742	1.221
Detection sensitivity (dB)	0.46	0.78	0.67

shown in Fig. 5(c), which means the diameter of delamination area could be predicted by the above formulas.

3.3. Detection sensitivity of delamination thickness by ΔS_{21} (dB)

The delamination thickness is another critical quantitative index for evaluating the damage and service life of CFRP composites. Fig. 6(a) shows the fabrication process of the CFRPs with different delamination thicknesses, which were reproduced using the insertion of 0.2 mm and 0.4 mm thick Teflon films.

As discussed in the previous section, the lower detection sensitivity

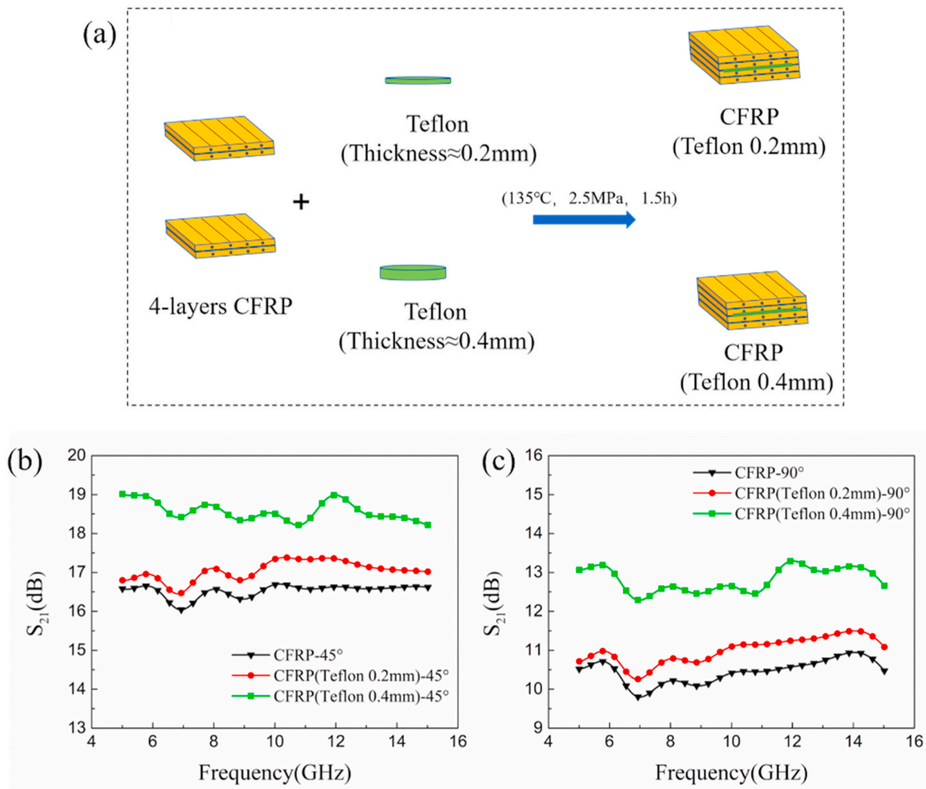

Fig. 6. (a) Preparation process of CFRP inserted with different thicknesses of Teflon film; (b) (c) SE values at the incident angles of 45° and 90°.

at the fiber direction was mainly due to the smaller skin depth and poor transmit ability of the EM wave at the 0° incident angle, and thus, the detection sensitivity to the delamination thickness was investigated at the incident angles of 45° and 90°. A clear difference in SE value could be observed in the entire frequency range of 5–15 GHz as shown in Fig. 6 (b) and (c), where the SE value increased with the increment in delamination thickness. The largest detection sensitivity of the CFRP with a 0.4 mm delamination thickness was 2.23 dB as shown (Table 3), which means the sensitivity of the thickness change was around 5.6 dB/mm. Thus, it can be concluded that the delamination thickness inside CFRPs can be identified successfully by the EMW-NDT method at an incident angle of 45° and/or 90°.

3.4. Detection of crack damage

To investigate crack damage, a slit was reproduced in the unidirectional CFRP samples. Two types of slit, one vertical and one parallel to the fiber direction, were introduced. Fig. 7 (a) shows the SE results for the two slits. When EM waves penetrate into CFRP composites, the displacement current will be coupled to the surface of the CFRP to create a magnetic field perpendicular to the current, as shown in Fig. 7 (a). An electromotive force running opposite to the induced current is then formed, which is known as the "skin effect" [42]. The EM waves will be attenuated by this skin effect when penetrate through the CFRP composites. Therefore, the continuity of the induced current path plays a vital role in EMI shielding performance. When the electric field of the incident EM wave ran parallel to the carbon fiber direction (0°), the vertical slit blocked the current path of the CFRP and caused greater obstruction and discontinuity for the induced current than the parallel slit, as shown in Fig. 7(a). All of this caused the significant decrease in SE values with the existence of slits in the CFRP composites, with the vertical slit leading to more EM leakage, resulted in the lower SE values, as shown in Fig. 7(b). Thus, it can be concluded that both the slit and the slit orientation can be identified successfully at a 0° incident angle.

When the incident angles were 45° and 90°, an interesting result emerged in that the EMI SE values of the vertical-slit CFRP were higher than with the parallel-slit CFRP, as shown in Fig. 7(c) and (d), which was the opposite to the result at the 0° incident angle. This was because the incident angle between the slit and the electric field direction determined the EMI shielding performance of the CFRP. Taking the 90° incident angle as an example, the parallel-slit CFRP, in which the slit was perpendicular to the electric field of the EM waves, led to greater discontinuity of the incident current, which resulted in a lower SE value. In addition, the SE value difference between the vertical-slit CFRP and the parallel-slit CFRP at the 0° test angle was larger than that at the 90° incident angle, as shown in Fig. 7(b) and (d). It can be concluded that the EMW-NDT method could be applied to identify the slit orientation on the CFRP composites, while the attention must be paid to the evaluation criteria when using various incident angles.

Table 3
Detection sensitivity ΔS21 (dB) of delamination thickness at 10 GHz.

Specimen	45° testing angle		90° testing angle	
	S_{21}(dB)	ΔS_{21} (dB)	S_{21}(dB)	ΔS_{21} (dB)
CFRP	16.68	/	10.41	/
CFRP (Teflon 0.2 mm)	17.34	0.66 dB	11.09	0.69 dB
CFRP (Teflon 0.4 mm)	18.5	1.82 dB	12.64	2.23 dB

3.5. Detection sensitivity of slit length by ΔS_{21} (dB)

The influence of the slit length in the vertical-slit type was investigated. Here, vertical slits with various lengths (2, 6 and 10 cm) were introduced in the unidirectional CFRP, with the width of the slits around 0.1 mm, as shown in Fig. 8 (a). As Fig. 8 (b) shows, a clear difference in SE value with the slit length change was observed at the 0° incident angle, with strong peaks appearing at 10.2 GHz. Meanwhile, the best detection sensitivity appeared at the 0° incident angle under 8 GHz as

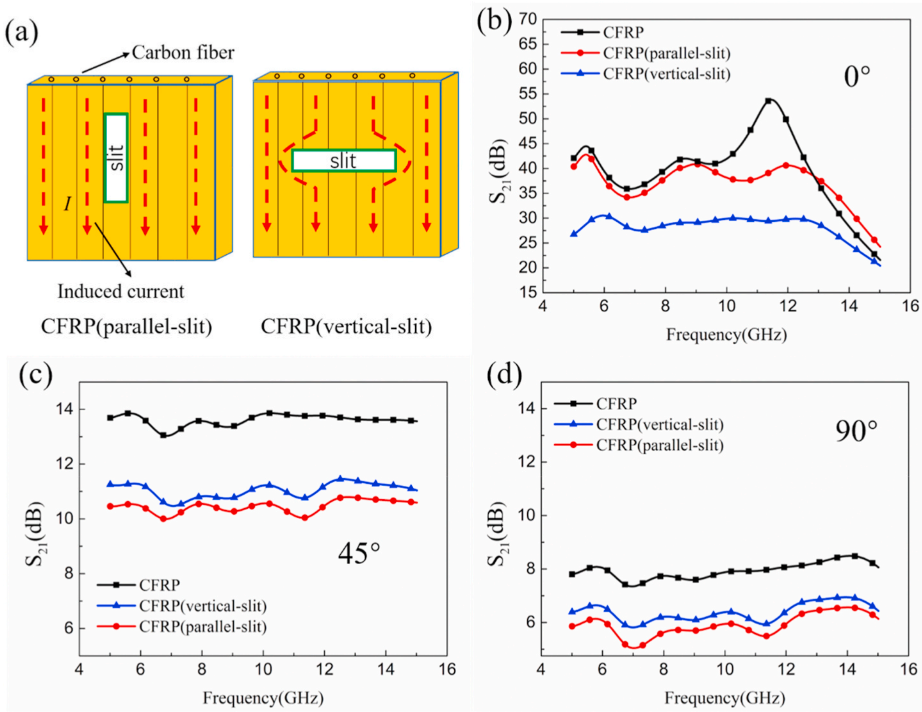

Fig. 7. (a) CFRPs with slits; SE values of the CFRPs at different incident angles of (b) 0°, (c) 45°, and (d) 90°.

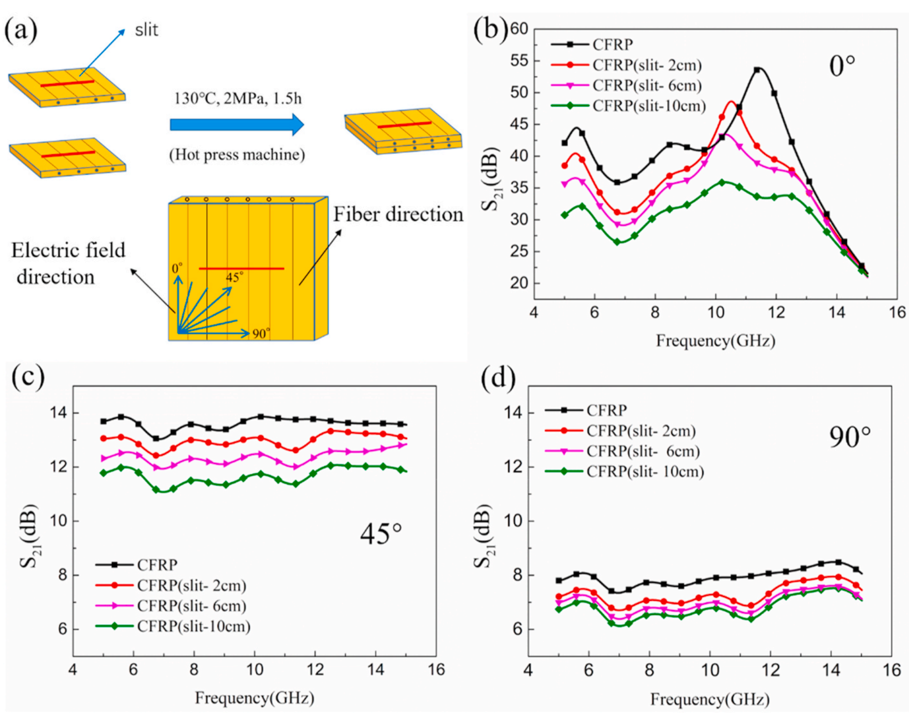

Fig. 8. (a) CFRP with slit; SE values of CFRP at different testing angles of (b) 0°, (c) 45°, and (d) 90°.

shown in Fig. 9. For the 45° and 90° incident angles, although their detection sensitivity was lower than that of the 0° incident angle (Fig. 8 (c), (d)), it was sufficient to determine the slit length of CFRP composite by the detection sensitivity. The results show that the detection sensitivity value increased almost linearly with the increment of the slit length (d), which can be expressed approximately by the linear equation as follows:

$$\Delta S_{21}(dB) = 0.611 \times d + 3.79 \text{for the } 0^\circ \text{ incident angle} \quad (16)$$

$$\Delta S_{21}(dB) = 0.179 \times d + 0.272 \text{for the } 45^\circ \text{ incident angle} \quad (17)$$

$$\Delta S_{21}(dB) = 0.066 \times d + 0.528 \text{for the } 90^\circ \text{ incident angle} \quad (18)$$

As shown in Fig. 9, the predicted detection sensitivity values by the above equations are in good consistent with the experimental result, that means the slit length could be predicted by the proposed formulas.

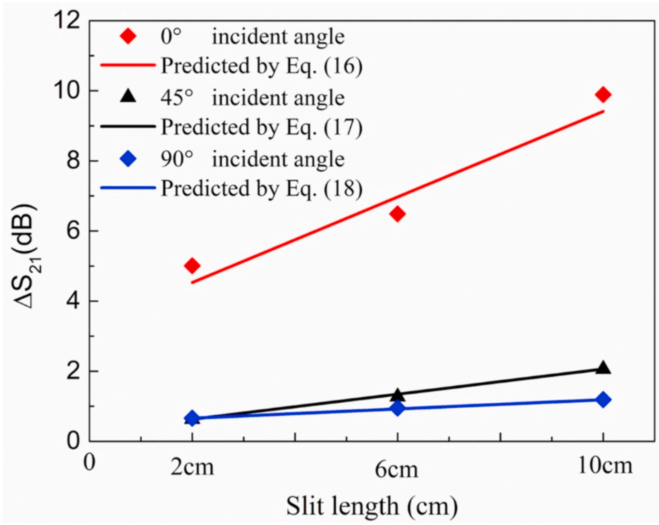

Fig. 9. Detection sensitivity of slit length at different incident angles under 8 GHz.

4. Conclusions

A novel NDT method (EMW-NDT) for assessing the damage in CFRP composites was presented in this study. The detection capacity of the EMW-NDT method in relation to the delamination and crack damage was investigated and identified systematically. Besides, the effect of the incident angle of the EM wave on the detection sensitivity for CFRPs was also comprehensively discussed. The results indicated that delamination damage with different sizes and thicknesses could be identified with high detection sensitivity using the proposed method. Then, a reasonable detection sensitivity in the damage volume change of delamination was confirmed, with the damage aera ratio of 12.6%/dB and a thickness change of 5.6 dB/mm. In terms of crack damage, both the slit and its length were detected, with the slit direction also identified successfully based on the characteristics of EMI shielding anisotropy in CFRPs. The result also shows that the incident angle of the EM wave plays a vital role in detection sensitivity due to the skin effect. The EMW-NDT method is based on the electromagnetic wave technique and is contactless, which means a coupling medium is not required in the detection process. It is proved that the proposed method can be applied to the damage detection of CFRP composites, which is both rapid and efficient. As such, the proposed EMW-NDT method exhibits vast potential for NDT application of CFRP composites and uses in various fields.

Author contributions

Qing-Qing Ni: Resources, Investigation, Data analysis, Writing - Review & Editing.
Jun Hong: Investigation, Experimental operation, Writing - Original Draft, Review & Editing.
Ping Xu: Experimental operation; Data analysis; Writing - Original Draft.
Zhenzhen Xu: Resources, Investigation.
Kirill Khvostunkov: Methodology, Resources.
Hong Xia: Methodology, Resources.

Declaration of competing interest

The authors declare that they have no known competing financial interests or personal relationships that could have appeared to influence the work reported in this paper.

Acknowledgment

This work was supported by the Japan Society for the Promotion of Science (JSPS KAKENHI 26420721) and National Natural Science Foundation of China (No.52073259). One of authors gratefully acknowledges financial support from the China Scholarship Abroad Fund (No.201608340069).

References

[1] H.A. Maples, O. Smith, C. Burgstaller, P. Robinson, A. Bismarck, Improving the ply/interleaf interface in carbon fibre reinforced composites with variable stiffness, Compos. Sci. Technol. 128 (2016) 185–192.
[2] Y.F. Zhu, L. Zhang, T. Natsuki, Y.Q. Fu, Q.Q. Ni, Facile synthesis of BaTiO3 nanotubes and their microwave absorption properties, ACS Appl. Mater. Interfaces 4 (2012) 2101–2106.
[3] T. Bergmann, S. Heimbs, M. Maier, Mechanical properties and energy absorption capability of woven fabric composites under ±45° off-axis tension, Compos. Struct. 125 (2015) 362–373.
[4] Q.Q. Ni, Y.F. Zhu, L.J. Yu, Y.Q. Fu, One-dimensional carbon nanotube@barium titanate@polyaniline multiheterostructures for microwave absorbing application, Nanoscale Res Lett 10 (2015) 174.
[5] C.-S. Zhang, Q.-Q. Ni, S.-Y. Fu, K. Kurashiki, Electromagnetic interference shielding effect of nanocomposites with carbon nanotube and shape memory polymer, Compos. Sci. Technol. 67 (2007) 2973–2980.
[6] L. Cheng, G.Y. Tian, Comparison of nondestructive testing methods on detection of delaminations in composites, Journal of Sensors 2012 (2012) 1–7.
[7] B. Salski, W. Gwarek, P. Korpas, S. Reszewicz, A.Y.B. Chong, P. Theodorakeas, I. Hatziioannidis, V. Kappatos, C. Selcuk, T.-H. Gan, M. Koui, M. Iwanowski, B. Zielinski, Non-destructive testing of carbon-fibre-reinforced polymer materials with a radio-frequency inductive sensor, Compos. Struct. 122 (2015) 104–112.
[8] D.D.L. Chung, Processing-structure-property relationships of continuous carbon fiber polymer-matrix composites, Mater. Sci. Eng. R Rep. 113 (2017) 1–29.
[9] W. Gong, J. Chen, E.A. Patterson, Buckling and delamination growth behaviour of delaminated composite panels subject to four-point bending, Compos. Struct. 138 (2016) 122–133.
[10] T. Yamane, A. Todoroki, Doublet analysis of changes in electric potential induced by delamination cracks in carbon-fiber-reinforced polymer laminates, Compos. Struct. 176 (2017) 217–224.
[11] J.C. Moulder, E. Uzal, J.H. Rose, Thickness and conductivity of metallic layers from eddy current measurements, Rev. Sci. Instrum. 63 (1992) 3455–3465.
[12] Z. Li, Z. Meng, A review of the radio frequency non-destructive testing for carbon-fibre composites, Meas. Sci. Rev. 16 (2016) 68–76.
[13] D. Wu, F. Cheng, F. Yang, C. Huang, Non-destructive testing for carbon-fiber-reinforced plastic (CFRP) using a novel eddy current probe, Compos. B Eng. 177 (2019) 107460.
[14] L.U. Daura, G. Tian, Q. Yi, A. Sophian, Wireless power transfer-based eddy current non-destructive testing using a flexible printed coil array, Philos Trans A Math Phys Eng Sci 378 (2020) 20190579.
[15] K. Mizukami, A.S.b. Ibrahim, K. Ogi, N. Matvieieva, I. Kharabet, M. Schulze, H. Heuer, Enhancement of sensitivity to delamination in eddy current testing of carbon fiber composites by varying probe geometry, Compos. Struct. 226 (2019) 111227.
[16] Y. He, G. Tian, M. Pan, D. Chen, Non-destructive testing of low-energy impact in CFRP laminates and interior defects in honeycomb sandwich using scanning pulsed eddy current, Compos. B Eng. 59 (2014) 196–203.
[17] K. Mizukami, Y. Mizutani, A. Todoroki, Y. Suzuki, Analytical solutions to eddy current in carbon fiber-reinforced composites induced by line current, Adv. Compos. Mater. 25 (2015) 385–401.
[18] S. Jiao, J. Li, F. Du, L. Sun, Z. Zeng, Characteristics of eddy current distribution in carbon fiber reinforced polymer, Journal of Sensors 2016 (2016) 1–8.
[19] A.M. Amaro, P.N.B. Reis, M.F.S.F. de Moura, J.B. Santos, Damage detection on laminated composite materials using several NDT techniques, Insight - Non-Destructive Testing and Condition Monitoring 54 (2012) 14–20.
[20] Q. Shen, M. Omar, S. Dongri, Ultrasonic NDE techniques for impact damage inspection on CFRP laminates, J. Mater. Sci. Res. 1 (2011).
[21] A.M. Amaro, J.B. Santos, J.S. Cirne, Delamination depth in composites laminates with interface elements and ultrasound analysis, Strain 47 (2011) 138–145.
[22] M. Kersemans, A. Martens, K. Van Den Abeele, J. Degrieck, F. Zastavnik, L. Pyl, H. Sol, W. Van Paepegem, Detection and localization of delaminations in thin carbon fiber reinforced composites with the ultrasonic polar scan, J. Nondestr. Eval. 33 (2014) 522–534.
[23] M. Kusano, H. Hatano, M. Watanabe, S. Takekawa, H. Yamawaki, K. Oguchi, M. Enoki, Mid-infrared pulsed laser ultrasonic testing for carbon fiber reinforced plastics, Ultrasonics 84 (2018) 310–318.
[24] Jan-Carl Grager, Daniel Kotschate, Jakob Gamper, Mate Gaal, Katja Pinkert, Mooshofer Hubert, Matthias Goldammer, C.U. Grosse, in: 12th European Conference on Non-destructive Testing, Gothenburg, Sweden, 2018.
[25] Y.Y. Hung, Applications of digital shearography for testing of composite structures, Compos. B Eng. 30 (1999), 765-733.
[26] V. Pagliarulo, V. Lopresto, A. Langella, V. Antonucci, M.R. Ricciardi, P. Ferraro, Non-destructive Evaluation of Impact Damage on Carbon Fiber Laminates: Comparison between ESPI and Shearography, vol. 1740, 2016, 040002.

[27] C. Goidescu, H. Welemane, C. Garnier, M. Fazzini, R. Brault, E. Péronnet, S. Mistou, Damage investigation in CFRP composites using full-field measurement techniques: combination of digital image stereo-correlation, infrared thermography and X-ray tomography, Compos. B Eng. 48 (2013) 95–105.
[28] T. Mathieu, R. Véronique, L. Nicolas Ducros, Verger, in: 11th European Conference on Non-destructive Testing (ECNDT 2014), Prague, Czech Republic, 2014.
[29] S. Gholizadeh, A review of non-destructive testing methods of composite materials, Procedia Structural Integrity 1 (2016) 50–57.
[30] C.Q. Wu, W.P. Wang, Q.G. Yuan, Y.J. Li, W. Zhang, X.D. Zhang, Infrared thermography non-destructive testing of composite materials, Adv. Mater. Res. 291–294 (2011) 1307–1310.
[31] R. Sutthaweekul, G. Tian, Z. Wang, F. Ciampa, Microwave open-ended waveguide for detection and characterisation of FBHs in coated GFRP pipes, Compos. Struct. 225 (2019) 111080.
[32] V.P. Vavilov, Modeling and characterizing impact damage in carbon fiber composites by thermal/infrared non-destructive testing, Compos. B Eng. 61 (2014) 1–10.
[33] R. Steinberger, T. Valadasleitao, E. Ladstatter, G. Pinter, W. Billinger, R. Lang, Infrared thermographic techniques for non-destructive damage characterization of carbon fibre reinforced polymers during tensile fatigue testing, Int. J. Fatig. 28 (2006) 1340–1347.
[34] C. Meola, S. Boccardi, G.M. Carlomagno, N.D. Boffa, E. Monaco, F. Ricci, Nondestructive evaluation of carbon fibre reinforced composites with infrared thermography and ultrasonics, Compos. Struct. 134 (2015) 845–853.
[35] D.K. Ghodgaonkar, V.V. Varadan, V.K. Varadan, A free-space method for measurement of dielectric constants and loss tangents at microwave frequencies, IEEE Transactions on Instrumentation and Measurement 38 (1989) 789–793.
[36] V.V. Varadan, R.D. Hollinger, D.K. Ghodgaonkar, V.K. Varadan, Free-space, broadband measurements of high-temperature, complex dielectric properties at microwave frequencies, IEEE Transactions on Instrumentation and Measurement 40 (1991) 842–846.
[37] U.C. Hasar, Non-destructive testing of hardened cement specimens at microwave frequencies using a simple free-space method, NDT E Int. 42 (2009) 550–557.
[38] M. Ozturk, U.K. Sevim, O. Akgol, M. Karaaslan, E. Unal, An electromagnetic non-destructive approach to determine dispersion and orientation of fiber reinforced concretes, Measurement 138 (2019) 356–367.
[39] R.H. Knibbs, J.B. Morris, The effects of fibre orientation on the physical properties of composites, Composites 5 (1974) 209–218.
[40] A. Todoroki, Electric current analysis for thick laminated CFRP composites, Trans. Jpn. Soc. Aeronaut. Space Sci. 55 (2011) 237–243.
[41] Richard B. Schulz, V.C. Plantz, D.R. Brush, Electromagnetic shielding theory and practice, IEEE Trans. Electromagn C. 30 (1988) 187–201.
[42] G.M. Kunkel, Shielding of Electromagnetic Waves Theory and Practice, Springer, Springer Nature Switzerland AG, Cham, 2020.